Environmental Research 295 (2026) 123996

Contents lists available at ScienceDirect

Environmental Research

journal homepage: www.elsevier.com/locate/envres

Climate warming drives nonlinear shifts in mercury bioavailability and ecological risk in coastal sediments

Yang-Guang Gu [a,e,*], Yanpeng Gao [b], Richard W. Jordan [c], Shi-Jun Jiang [d]

[a] South China Sea Fisheries Research Institute, Chinese Academy of Fishery Sciences, Guangzhou, 510300, China
[b] Institute of Environmental Health and Pollution Control, Guangdong University of Technology, Guangzhou, 510006, China
[c] Faculty of Science, Yamagata University, Yamagata, 990-8560, Japan
[d] State Key Laboratory of Marine Resource Utilization in South China Sea, Hainan University, Haikou, 570228, China
[e] Key Laboratory of Fishery Ecology and Environment, Guangdong Province, Guangzhou, 510300, China

ARTICLE INFO

Keywords:
Methylmercury (MeHg)
Inorganic mercury (InHg Hg^{2+})
Diffusive gradients in thin films (DGT)
Ecotoxicological risk
Temperature-dependent bioavailability
Daya Bay

ABSTRACT

Mercury (Hg) contamination poses urgent ecotoxicological concerns for coastal ecosystems, yet the temperature-dependent bioavailability and ecotoxicological risks of different Hg species remain poorly understood. Here, we investigated how warming influences methylmercury (MeHg) and divalent inorganic mercury (InHg, Hg^{2+}) in coastal sediments using diffusive gradients in thin films (DGT) to capture labile, bioavailable Hg. DGT provides a dynamic, environmentally relevant measure of Hg accessibility, integrating diffusion, adsorption, and complexation processes that regulate exposure to benthic organisms. To quantify ecological consequences, we applied the SPI (Species Sensitivity Distribution–Probabilistic Risk Assessment–Inclusion-Exclusion Principle) model, enabling evaluation of both individual and joint ecotoxicological risks. Our framework reveals nonlinear, species-specific responses of Hg bioavailability and ecotoxicological risk to rising sediment temperatures, with MeHg overwhelmingly dominating total risk, while InHg contributes modestly yet meaningfully. These findings establish a mechanistic and predictive approach for assessing temperature-sensitive Hg behavior and ecotoxicological outcomes in coastal sediments, providing critical insights for climate-adaptive risk assessment and proactive environmental management.

1. Introduction

Mercury (Hg) contamination poses a persistent threat to coastal ecosystems due to its toxicity, bioaccumulation, and potential for biomagnification (Jonsson et al., 2017; Blanchfield et al., 2022; Lan et al., 2025; Lavergne et al., 2025). Among Hg species, methylmercury (MeHg) is highly bioavailable and readily accumulates in aquatic food webs, whereas divalent inorganic mercury (InHg, Hg^{2+}) generally exhibits lower mobility but can still contribute to ecotoxicological risk under specific environmental conditions (Park and Zheng, 2012; Jonsson et al., 2017; Harding et al., 2018; Gu et al., 2022b; Saiz-Lopez et al., 2025). Sediments act as both a sink and secondary source of these species, with bioavailability controlled by the interplay of diffusion, adsorption, and complexation processes (Bolaños-Alvarez et al., 2024; Rosati et al., 2024; Méndez-López et al., 2025). Despite the recognized importance of temperature in influencing these processes, quantitative understanding of how warming regulates the bioavailability and ecotoxicological risk of both MeHg and InHg remains limited (Dastoor et al., 2022; Rosati et al., 2024).

Global climate warming is altering sediment thermal regimes in coastal and estuarine systems, potentially affecting Hg speciation, mobility, and ecotoxicological outcomes (Jonsson et al., 2017; Gu et al., 2026; Li et al., 2025a, 2025b; Zhong et al., 2025). Temperature can influence both diffusion kinetics and the stability of Hg-ligand complexes, dynamically regulating the fraction of labile Hg accessible to benthic organisms (Haitzer et al., 2002; Buckman et al., 2019; Pi et al., 2020; Wang et al., 2020). These effects are often nonlinear and species-specific, reflecting the complex interplay of kinetic and thermodynamic controls (Miller et al., 2009; Liem-Nguyen et al., 2017; Olsen et al., 2018; Helmrich et al., 2022). Current studies rarely capture such non-monotonic responses and frequently focus on a single Hg species, limiting mechanistic understanding of differential ecological implications under warming scenarios (Jonsson et al., 2017; Helmrich et al., 2022).

* Corresponding author. South China Sea Fisheries Research Institute, Chinese Academy of Fishery Sciences, Guangzhou, 510300, China.
E-mail address: hydrobio@163.com (Y.-G. Gu).

https://doi.org/10.1016/j.envres.2026.123996
Received 12 December 2025; Received in revised form 5 February 2026; Accepted 7 February 2026
Available online 9 February 2026

To address these knowledge gaps, we measured DGT-labile MeHg and InHg in sediments across a range of temperatures. Diffusive gradients in thin films (DGT) is a passive *in situ* technique that mimics metal uptake by benthic organisms and selectively captures the labile Hg species most relevant to ecological risk (Davison and Zhang, 1994; Zhang and Davison, 1995; Gu et al., 2022b). Unlike total Hg measurements, DGT integrates the effects of diffusion, adsorption, and complexation in sediments, providing a dynamic and environmentally realistic assessment of bioavailability (Davison and Zhang, 1994; Zhang and Davison, 1995; Gu et al., 2022b). The measured DGT-labile Hg concentrations were incorporated into the SPI (Species Sensitivity Distribution–Probabilistic Risk Assessment–Inclusion-Exclusion Principle) model, a novel framework that quantifies both individual and joint ecotoxicological risks of multiple pollutants (Gu et al., 2020, 2022a, 2025a, 2026). By combining DGT-based bioavailability measurements with SPI modeling, this approach systematically evaluates temperature-driven, species-specific variations in Hg bioavailability and ecotoxicological risk, highlighting the dominant role of MeHg and the weaker yet non-negligible contributions of InHg in coastal sediments.

This study focuses on Daya Bay, a thermally influenced coastal system in the northern South China Sea, providing a representative setting to examine how sediment temperature modulates Hg behavior and associated ecotoxicological risks. By integrating DGT measurements with SPI modeling, this work establishes a mechanistic and predictive framework to assess nonlinear, temperature-dependent responses of MeHg and InHg, offering novel insights into climate-sensitive contaminant dynamics and supporting improved risk assessment under warming scenarios.

2. Materials and methods

2.1. Study area

Daya Bay is a shallow, semi-enclosed drowned-valley bay covering approximately 516 km^2, with water depths ranging from 5 to 18 m (Gu et al., 2023, 2026). The bay experiences a subtropical marine climate, with an average annual temperature of 21.7 °C, mean annual rainfall of 1984.4 mm, and relative humidity around 82% (Gu et al., 2022b, 2026). Only three small rivers discharge into the bay, while most water exchange occurs with the South China Sea (Fig. S1).

Daya Bay was selected as the study site due to its pronounced exposure to both natural and anthropogenic influences (Gu et al., 2023, 2025b). The region is strongly affected by rapid urbanization and economic development in Shenzhen—one of China's most dynamic coastal cities—and by intensive industrial activities from the adjacent Huizhou Daya Bay petrochemical complex (Gu et al., 2022b, 2023, 2025b, 2026). Thermal discharges from the Daya Bay Nuclear Power Plant further modify local hydrodynamics and water temperatures. Previous studies in surface sediments of Daya Bay have shown that rising temperatures decrease the bioavailability and ecotoxicological risk of rare earth elements (Gu et al., 2026). The bay is also significantly influenced by trace metal inputs from both natural and anthropogenic sources, primarily via sewage discharge, surface runoff, and atmospheric deposition (Gu et al., 2012; Man et al., 2022, 2025).

Based on these characteristics, surface sediments of Daya Bay provide an ideal setting to investigate how rising temperatures under global climate change influence the bioavailability and ecotoxicological risks of methylmercury and inorganic mercury, as well as their individual and combined effects on aquatic biota.

2.2. Sampling and DGT experiment

In this study, two surface sediment samples were collected from each of the 24 sites in Daya Bay, South China, in January 2020 (Fig. S1), ensuring spatial representativeness across the bay. The particle size composition of the surface sediments has been reported in detail in our previous study, where silt was identified as the dominant fraction, followed by varying proportions of clay and sand (Gu et al., 2026). One set of 24 sediment samples was thoroughly mixed on-site and immediately sealed in polyethylene bags for subsequent DGT experiments. Both sediment and overlying seawater samples were stored in insulated boxes with ice (<4 °C) to minimize physicochemical changes during transportation to the laboratory.

In the laboratory, the homogenized sediments were transferred into 2 L light-proof polyvinyl chloride (PVC) containers, each filled with 500 mL of pre-collected Daya Bay seawater maintained at low temperature. To investigate the temperature-dependent bioavailability of mercury species (MeHg and InHg), five temperature gradients (0 °C, 10 °C, 20 °C, 30 °C, and 40 °C) were established. The selected temperature range was designed to encompass ambient conditions and extended thermal scenarios for mechanistic evaluation, rather than to directly replicate *in situ* temperatures. Three replicates were prepared for each temperature condition to ensure reliability and reproducibility. All samples were incubated in temperature-controlled chambers for 96 h to maintain stable thermal conditions.

Following incubation, flat-type DGT devices (TCH-95 DGT probes, EasySensor Ltd., Nanjing, China) equipped with Chelex binding gels were vertically inserted into each sediment container and deployed for 48 h to capture the *in situ* diffusion and resupply dynamics of MeHg and InHg. After retrieval, the DGT devices were gently rinsed with ultrapure water to remove attached particles and then sealed in moisture-retaining bags for transport.

For quantitative analysis, each DGT binding gel was sectioned into 4.0 mm slices using a precision ceramic-blade cutter (EasySensor Ltd., Nanjing, China). Each DGT binding gel slice was eluted separately with 10 mL of an eluent containing 0.1 mol/L HCl and 2% thiourea for 24 h prior to analysis, following the method described by Ren et al. (2018), and the eluates were analyzed for MeHg and InHg concentrations by cold vapor atomic fluorescence spectrometry (CV-AFS).

2.3. Quality assurance and quality control (QA/QC) for Hg species analysis

Procedural blanks were routinely analyzed and were consistently below detection limits. Analytical precision was assessed using replicate DGT deployments and repeated measurements. The relative standard deviations (RSDs) of MeHg ranged from 2.0% to 9.2%, and those of InHg ranged from 2.0% to 7.8% across all temperature treatments, demonstrating satisfactory reproducibility. In addition, an internal standard recovery test was conducted by spiking parallel sediment samples with 0.5 μg/L and 1.0 μg/L of InHg and MeHg, respectively. The recovery rates were 97.6–100.4% for InHg and 98.8–101.2% for MeHg, confirming the accuracy of the analytical procedure.

Method detection limits (MDLs) for MeHg and InHg were 0.01 and 0.02 μg/L, respectively, determined following standard procedures, and were comparable to those reported in previous DGT-based Hg studies (Ren et al., 2018; Gu et al., 2022b). Overall, these QA/QC measures ensured the reliability, accuracy, and robustness of the analytical results. All DGT preparation, deployment, and analytical procedures were performed under standardized laboratory conditions at EasySensor Ltd. (Nanjing, China).

2.4. Formulas for DGT-labile concentrations

The diffusion of mercury species (MeHg and InHg) through the diffusive gel layer in DGT devices follows Fick's first law. The concentrations measured in the DGT eluate were first transformed into the accumulated mass of the analyte (M) according to Eq. (1):

$$M = \frac{C_e(V_e + V_g)}{f_e} \quad (1)$$

where C_e denotes the mercury species concentration in the elution solution (μg/L), V_e is the volume of the eluent, V_g represents the combined volume of the extract and gel (mL), and f_e is the elution efficiency factor of the specific mercury species.

The corresponding DGT-labile mercury species concentration (C_{DGT}) was then calculated using Eq. (2):

$$C_{DGT} = \frac{M \triangle g}{DAt} \tag{2}$$

where $\triangle g$ is the thickness of the diffusive layer (cm), D is the diffusion coefficient of each mercury species within the gel at the measured temperature (cm^2/s), A is the exposed surface area of the DGT device (cm^2), and t is the deployment time (96 h in this study).

2.5. SPI model framework for probabilistic and combined ecotoxicological risk assessment

The SPI (SSD–PRA–IEP) model, originally proposed by Gu et al. (2020, 2022a, 2025a, 2026), provides a unified probabilistic framework capable of assessing both individual and cumulative ecological risks of pollutants in aquatic ecosystems. In this study, the SPI model was applied to quantify the temperature-dependent risks of single mercury species (MeHg and InHg) as well as their combined effects on aquatic biota. The framework integrates species sensitivity distribution (SSD), probabilistic risk assessment (PRA), and the inclusion–exclusion principle (IEP), thereby enabling a consistent evaluation of pollutant-specific and multi-pollutant risks while avoiding overestimation arising from overlapping effects (Fig. S2).

2.5.1. Step 1: pollutant concentration and toxicity data

Bioavailable concentrations of target pollutants were determined using the diffusive gradients in thin films (DGT) technique. Acute and chronic toxicity data were collected from the USEPA ECOTOX database (https://www.epa.gov/ecotox) and peer-reviewed publications from ScienceDirect, Springer, Wiley Online Library, CNKI, and Google Scholar. The compiled dataset covered multiple trophic levels, including algae, crustaceans, fish, and mollusks. Detailed toxicity endpoints and species data are provided in Tables S1–S5.

2.5.2. Step 2: probabilistic risk assessment for single pollutants

For each pollutant, SSDs were constructed using the toxicity dataset, and probability density functions (PDFs) were generated to represent environmental exposure distributions. The single-pollutant ecological risk, expressed as the potentially affected fraction (PAF), was calculated by quantifying the overlap between the SSD and exposure PDFs. This probability represents the fraction of species that may be adversely affected when environmental concentrations exceed toxicity thresholds.

2.5.3. Step 3: combined ecotoxicological risk assessment

For multiple pollutants, the SPI model applies the IEP to integrate overlapping toxic probabilities. The cumulative ecological risk probability, $\Phi(A_1 + A_2 + \ldots + A_n)$, representing the likelihood that at least one pollutant induces adverse effects, is given by:

$$\Phi(A_1 + A_2 + \ldots + A_n) = \sum_{i=1}^{n} \Phi(A_i) - \sum_{i_1 < i_2} \Phi(A_{i_1} A_{i_2}) + \ldots + (-1)^{r+1} \sum_{i_1 < \ldots < i_r} \Phi(A_{i_1} \ldots A_{i_r}) + \ldots + (-1)^{n+1} \Phi(A_1 \ldots A_n) \tag{3}$$

where Φ denotes the probability of ecological impact from single or joint pollutants. This alternating-sum structure accounts for overlapping toxic effects and reduces bias in cumulative risk estimation.

2.6. Normalization and data processing for comparative visualization

To enable direct comparison between temperature-dependent variations in mercury bioavailability and ecological risk, both parameters were normalized onto a unified, dimensionless scale (0-1) (section 4.1). This normalization facilitates mechanistic interpretation of how kinetic-thermodynamic controls on mercury mobility (quantified by DGT) correspond to probabilistic ecological effects (modeled using the SPl framework) (section 4.1).

2.6.1. Normalization of relative bioavailability

The temperature-dependent bioavailable concentrations of mercury species were determined using the DGT technique. For each temperature T, the relative bioavailability ($R_{bio}(T)$) was calculated as:

$$R_{bio}(T) = \frac{C_{DGT}(T)}{C_{DGT}^{max}} \tag{4}$$

where $C_{DGT}(T)$ represents the DGT-labile concentration of a given mercury species (MeHg or InHg) at temperature T, and C_{DGT}^{max} is the maximum concentration observed among all temperature treatments. This normalization scales DGT-derived responses between 0 and 1, thereby emphasizing relative enhancement or suppression of mercury mobility under different thermal conditions.

2.6.2. Normalization of ecotoxicological risk probability

Ecological risk probabilities were computed using the SPl (SSD-PRA-IEP) framework described in section 2.5. For each temperature, the single-pollutant risk probability ($R_{risk}(T)$) corresponds to the potentiallyaffected fraction (PAF) derived from the overlap between the SSD and environmental exposureprobability density functions:

$$R_{risk}(T) = P(C_{DGT}(T) > HC_5) \tag{5}$$

where HC_5, denotes the hazardous concentration that protects 95% of species. To facilitate comparison with normalized DGT data, each risk probability was further scaled by its maximum value:

$$R_{eco}(T) = \frac{R_{risk}(T)}{R_{risk}^{max}} \tag{6}$$

yielding the normalized ecological risk probability ($R_{eco}(T)$).

2.6.3. Comparative visualization

Both normalized indicators, $R_{bio}(T)$ and $R_{eco}(T)$, were plotted against temperature on a single vertical axis labeled "Normalized relative bioavailability and ecological risk (0-1)". This co-visualization approach enables direct comparison between mechanistic (DGT-based) and ecotoxicological (SPl-based) thermal responses, highlighting their nonlinear temperature dependencies and species-specific sensitivities. Such normalization and coupling of bioavailability and ecological-risk profiles have been widely applied in integrated ecotoxicological assessments. Such normalization and coupling of bioavailability and ecological-risk profiles have been widely applied in integrated ecotoxicological assessments (Semenzin et al., 2008; OECD, 2017).

2.7. Statistical analysis

To examine the distributional characteristics of the dataset, the Kolmogorov–Smirnov (K–S) test was applied individually to the DGT-labile concentrations of each mercury species and to the toxicity dataset. The results revealed that, after logarithmic transformation, both mercury species concentrations and toxicity data conformed to a normal distribution pattern (Table S6). All K–S tests were performed using SPSS version 19.0 (IBM Corp., USA), whereas the overlap proportions between exposure and toxicity probability distributions were quantified with R software version 4.3.2 (64-bit, Windows platform).

3. Results

3.1. Temperature dependence of methylmercury (MeHg)

The DGT-labile MeHg concentration exhibited a clear nonlinear response to temperature (Fig. 1). The relationship was well described by a quadratic regression ($y = 4.158\text{-}0.201x + 0.00296x^2$, $R^2 = 0.998$), showing a pronounced decrease from 0 to 30 °C followed by a slight increase at 40 °C. The model predicts a minimum concentration near 34 °C, suggesting that the interplay between diffusion kinetics and ligand complexation may reach a thermodynamic equilibrium at this temperature (Supplementary section 1.1).

This temperature-dependent pattern likely reflects intrinsic changes in MeHg speciation and mobility within sediments, driven by the competing influences of diffusion kinetics and chemical complexation (Gabriel and Williamson, 2004; Bełdowski et al., 2018; Acquavita et al., 2021). At lower temperatures (0–20 °C), increased water viscosity and reduced molecular energy slow the diffusion of MeHg species and limit their release from solid phases into porewaters. As temperature rises, enhanced molecular motion accelerates the desorption and transport of MeHg from sediment particles, leading to greater porewater mobility (Buckman et al., 2019; Dabré et al., 2025). However, at temperatures exceeding ~30 °C, the stability of MeHg–thiol complexes may decline, facilitating ligand exchange and partial dissociation from organic or sulfide binding sites, thereby increasing the proportion of free or weakly complexed MeHg (Ullrich et al., 2001; Ravichandran, 2004). The overall nonlinear response—an initial decrease followed by a mild increase—thus represents the balance between diffusion-controlled release and thermodynamic destabilization of MeHg complexes under elevated temperatures.

3.2. Temperature dependence of inorganic mercury (InHg)

The DGT-labile inorganic mercury (InHg) concentration exhibited a non-monotonic response to temperature variation (0–40 °C), displaying an overall oscillatory–attenuating pattern rather than a simple linear trend (Fig. 2). The measured InHg concentrations were 0.366 ± 0.019, 0.869 ± 0.017, 0.237 ± 0.018, 0.524 ± 0.037, and 0.471 ± 0.022 μg/L at 0, 10, 20, 30, and 40 °C, respectively. Specifically, the concentration sharply increased from 0 to 10 °C, dropped markedly at 20 °C, partially recovered at 30 °C, and slightly declined at 40 °C. Such a non-monotonic pattern reflects the dynamic interplay between temperature-dependent

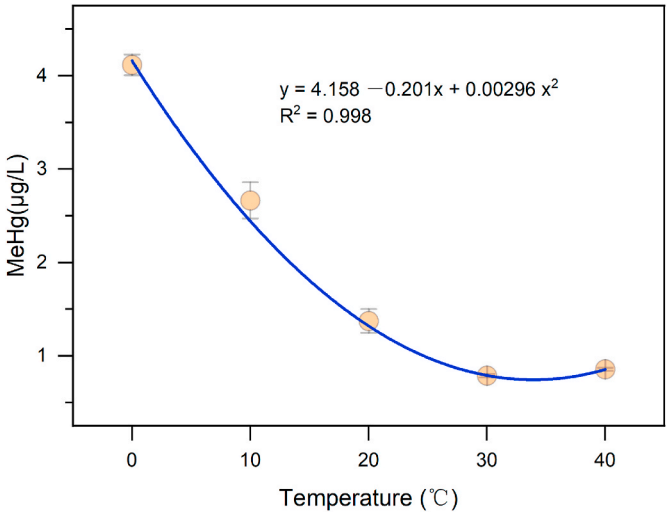

Fig. 1. Temperature-dependent variation in DGT-labile methylmercury concentration in coastal sediments. The error bars indicate ±1 SD of the measured values.

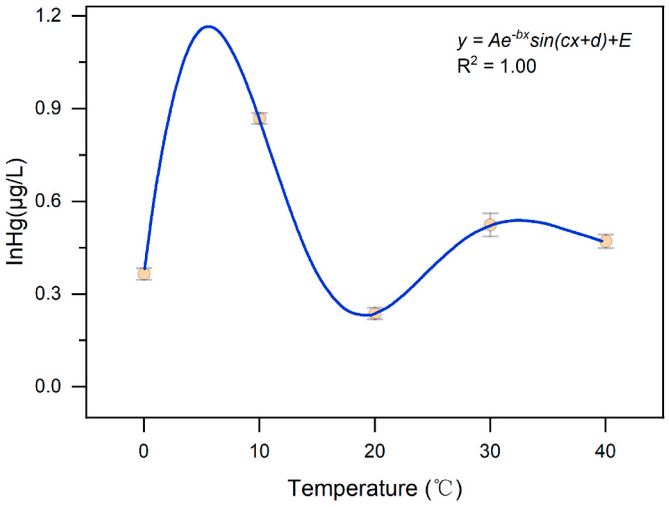

Fig. 2. Temperature-dependent variation of DGT-labile InHg described by a damped sinusoidal fit. The observed oscillatory–attenuating behavior indicates the interplay between temperature-driven diffusion enhancement and shifts in complexation equilibria of InHg species within the DGT interface. The error bars indicate ±1 SD of the measured values.

diffusion and the complexation equilibria of Hg species that jointly govern Hg transport and binding processes within the DGT system. To quantitatively capture this complex temperature dependence, a damped sinusoidal function, commonly used to describe acoustic attenuation or oscillatory decay, was employed:

$$y = Ae^{-bx}\sin(cx + d) + E$$

where y represents the DGT-labile InHg concentration, x is the temperature (°C), A denotes the initial amplitude, b the damping coefficient, c the oscillation frequency, d the phase shift, and E the steady-state term. The fitted parameters were $A = 1.1905$, $b = 0.08255$, $c = 0.23359$, $d = -0.08274$, and $E = 0.46403$, yielding $R^2 = 1.000$. Although the perfect goodness of fit mainly reflects the limited number of experimental data points, the function effectively captures the alternating enhancement and suppression of measurable Hg concentrations with increasing temperature and should therefore be interpreted as a semi-empirical rather than mechanistic description.

Mechanistically, the initial rise from 0 to 10 °C can be attributed to thermally enhanced diffusion of Hg species and increased dissociation of labile complexes, which collectively promote Hg transport toward the DGT binding layer (Ullrich et al., 2001; Ravichandran, 2004). The subsequent decline at 20 °C likely reflects a temperature-induced shift in aqueous speciation equilibrium, favoring the formation of more stable or less labile Hg complexes and thereby reducing their effective mobility (Ullrich et al., 2001; Ravichandran, 2004). Further warming (20–30 °C) enhances interfacial exchange kinetics and diffusion rates, leading to partial recovery of the measurable InHg fraction, while the slight decrease observed at 40 °C suggests the onset of competing chemical or structural processes that moderate further mobilization (Ullrich et al., 2001; Ravichandran, 2004). Overall, this oscillatory−attenuating pattern highlights the coupled thermodynamic and kinetic controls on Hg speciation and mobility, providing new insight into the temperature sensitivity of DGT-measured inorganic Hg in aquatic systems.

3.3. Temperature-dependent probabilistic ecological risks of MeHg, InHg, and their joint effects

Based on the probabilistic risk probabilities derived from Figs. 3–5, the temperature-dependent variations were further fitted using nonlinear regression models. The probabilistic ecological risks of MeHg, InHg, and their combined effects on aquatic biota exhibited distinct

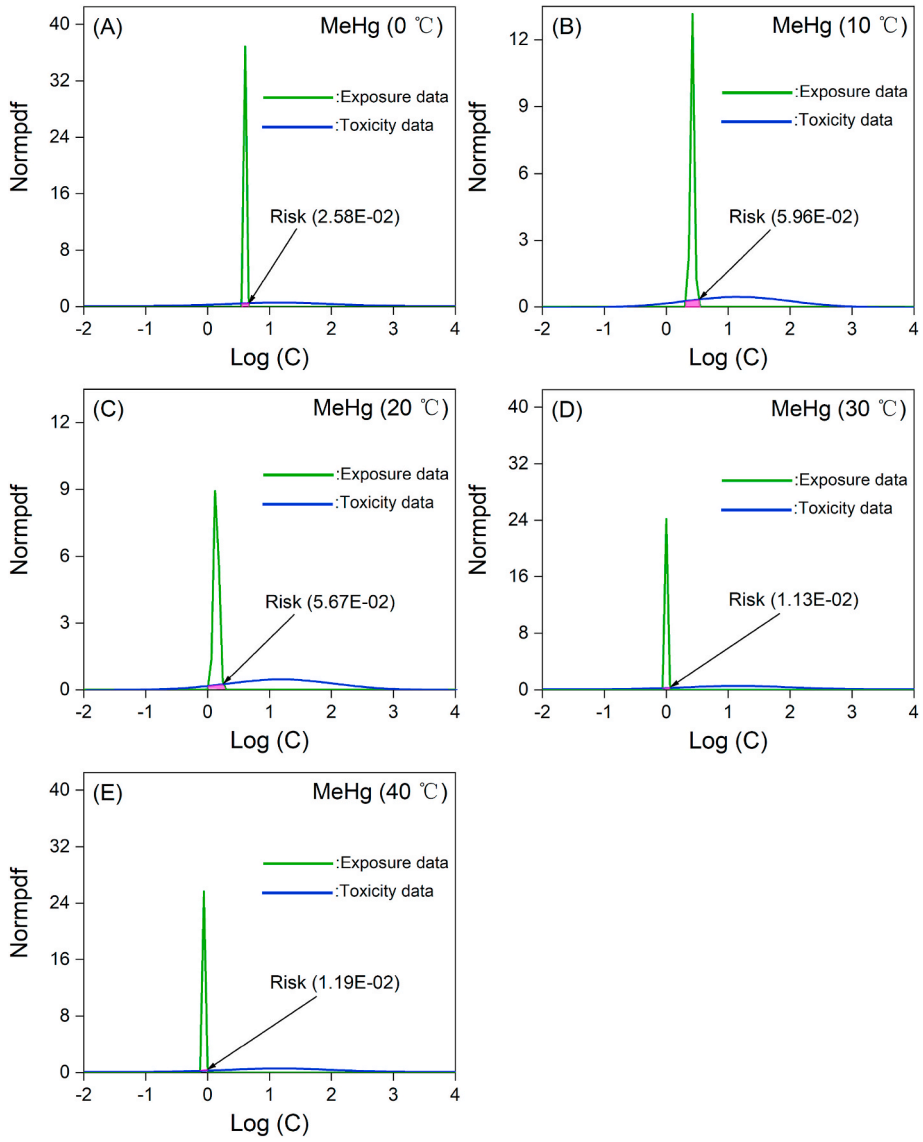

Fig. 3. Temperature-dependent probabilistic ecotoxicological risk of MeHg on aquatic biota at 0, 10, 20, 30, and 40 °C, estimated using the SPI model. Pink-shaded areas indicate ecotoxicological risk.

nonlinear responses to temperature (Fig. 6). Overall, these relationships were well captured by cubic polynomial regressions, indicating that the temperature dependence of ecological risk arises from coupled kinetic and thermodynamic controls on mercury speciation and bioavailability.

For MeHg, the ecological risk probability ($y = 6.89 \times 10^{-4}x^3 - 4.91 \times 10^{-2}x^2 + 0.828x + 2.445$, $R^2 = 0.943$) showed a pronounced nonlinear pattern, rising sharply from 0 to 10 °C (2.58 % → 5.96 %), remaining stable around 20 °C (5.67 %), and then decreasing markedly at higher temperatures (1.13 %–1.19 % between 30 and 40 °C). This trend mirrors the DGT-measured MeHg concentrations, suggesting that bioavailability-driven ecological effects are predominantly regulated by the competition between diffusion enhancement and complexation stability. At moderate temperatures, elevated molecular energy facilitates MeHg desorption and mobility, whereas beyond ~30 °C, partial dissociation of MeHg–thiol complexes likely alters speciation toward less bioavailable forms, leading to reduced ecological risk.

In contrast, InHg exhibited a weak and oscillatory temperature response ($y = -1.50 \times 10^{-5}x^3 + 8.36 \times 10^{-4}x^2 - 8.43 \times 10^{-3}x + 0.143$, $R^2 = 0.381$), with risk probabilities fluctuating narrowly between 0.11 % and 0.29 %. The low temperature sensitivity reflects the dominance of kinetically inert Hg–sulfide and Hg–organic complexes in sediments, which buffer InHg mobility and suppress temperature-induced variations in its labile fraction. Consequently, the ecological effect of InHg appears largely decoupled from thermally driven changes in its DGT-labile concentration.

The joint ecological risk of MeHg and InHg followed a similar nonlinear trajectory ($y = 6.81 \times 10^{-4}x^3 - 4.87 \times 10^{-2}x^2 + 0.823x + 2.588$, $R^2 = 0.952$), peaking at 10 °C (6.15 %) before declining at higher temperatures (1.36 % at 40 °C). The resemblance to the MeHg curve indicates that MeHg overwhelmingly dominates the total ecological risk of Hg mixtures, with InHg contributing only marginally to the combined effect. This dominance underscores the pivotal role of MeHg bioavailability in determining the overall temperature-dependent ecotoxicological outcomes of sedimentary mercury systems.

Collectively, these results reveal that temperature exerts a nonlinear and species-specific influence on mercury-related ecological risks. By quantitatively linking thermal variations to changes in diffusion dynamics and complexation equilibria, the present framework provides mechanistic insight into how environmental warming could modulate mercury bioavailability and ecological hazard in aquatic ecosystems.

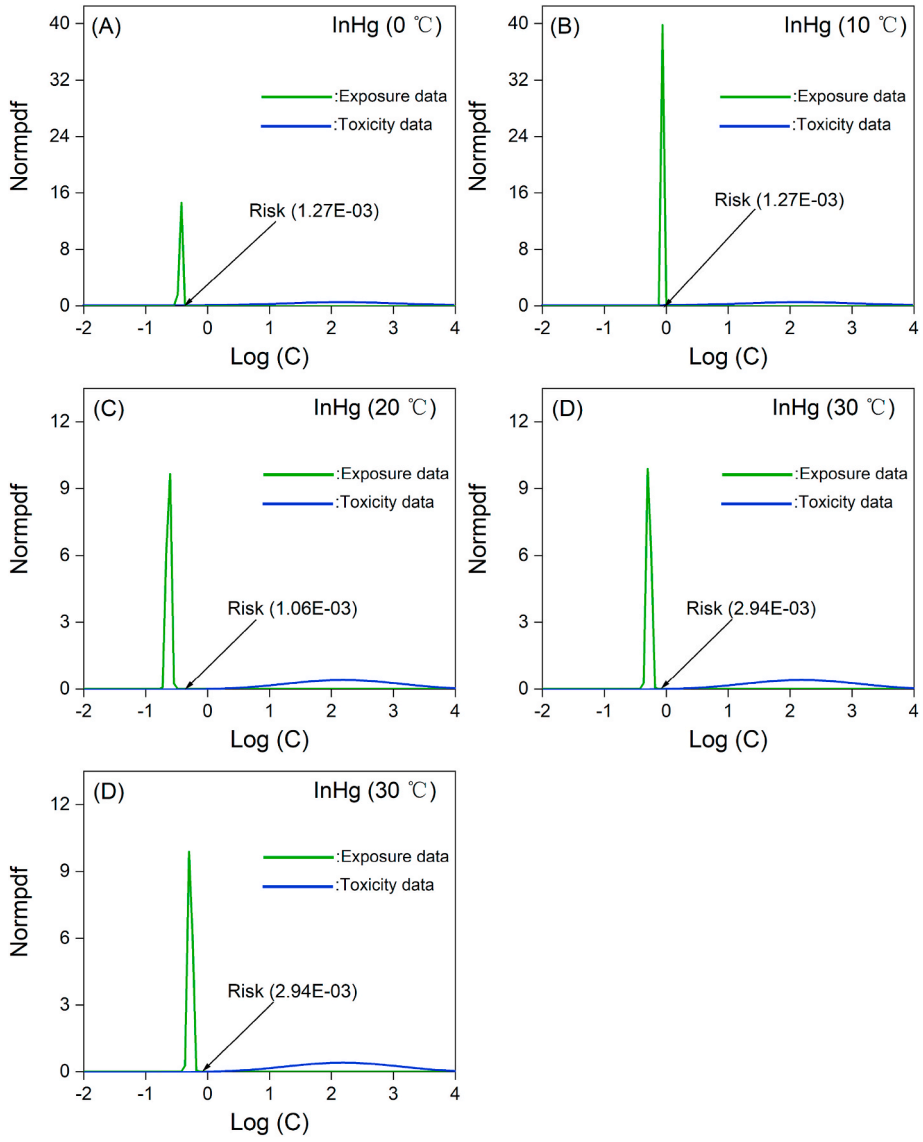

Fig. 4. Temperature-dependent probabilistic ecotoxicological risk of InHg on aquatic biota at 0, 10, 20, 30, and 40 °C, estimated using the SPI model. Pink-shaded areas indicate ecotoxicological risk.

4. Discussion

4.1. Temperature-modulated mercury speciation, bioavailability, and ecological implications

Temperature emerges as a pivotal environmental driver that modulates mercury mobility, speciation, and subsequent ecological risks in aquatic sediments (Fig. 7). The nonlinear responses observed in both MeHg and InHg concentrations, as well as their probabilistic risk profiles, highlight the complex coupling between kinetic diffusion processes and thermodynamic complexation equilibria. These temperature-dependent patterns indicate that even modest thermal shifts can substantially reconfigure the dynamic partitioning of mercury species between labile and inert phases, thereby altering their ecological accessibility (Fig. 7).

For MeHg, the pronounced parabolic and cubic responses suggest that thermal variation influences both its physicochemical behavior and its toxicological potential (Fig. 7). Moderate warming (10–20 °C) enhances MeHg diffusion and desorption from organic and sulfide binding sites, thereby increasing its DGT-labile fraction and risk probability (Fig. 7). Our observed temperature-dependent increase of labile MeHg at moderate warming (10–20 °C) is consistent with previous laboratory and field studies showing enhanced MeHg mobility under elevated temperatures (Liu et al., 2016; Ravichandran, 2004). However, excessive temperature (>30 °C) likely destabilizes thiol-bound MeHg species, leading to ligand exchange or re-adsorption onto sedimentary particles, effectively reducing the proportion of bioavailable MeHg (Fig. 7). The subsequent decline at higher temperatures (>30 °C) aligns with reported thermal destabilization of Hg–thiol complexes (Ullrich et al., 2001), further supporting the mechanistic interpretation of temperature-modulated Hg bioavailability. This temperature-induced shift between enhanced mobility and complexation stabilization underscores the dual control of kinetic and equilibrium processes on MeHg bioavailability.

In contrast, InHg demonstrates limited temperature sensitivity, reflecting its strong affinity for reduced sulfur ligands and its slower transformation dynamics (Fig. 7). The weak correspondence between InHg concentrations and ecological risk probability suggests that its bioavailability remains largely constrained by sediment redox conditions rather than direct thermal effects. Nonetheless, transient fluctuations in InHg risk around 20–30 °C may arise from minor speciation rearrangements or enhanced exchange between aqueous and solid-

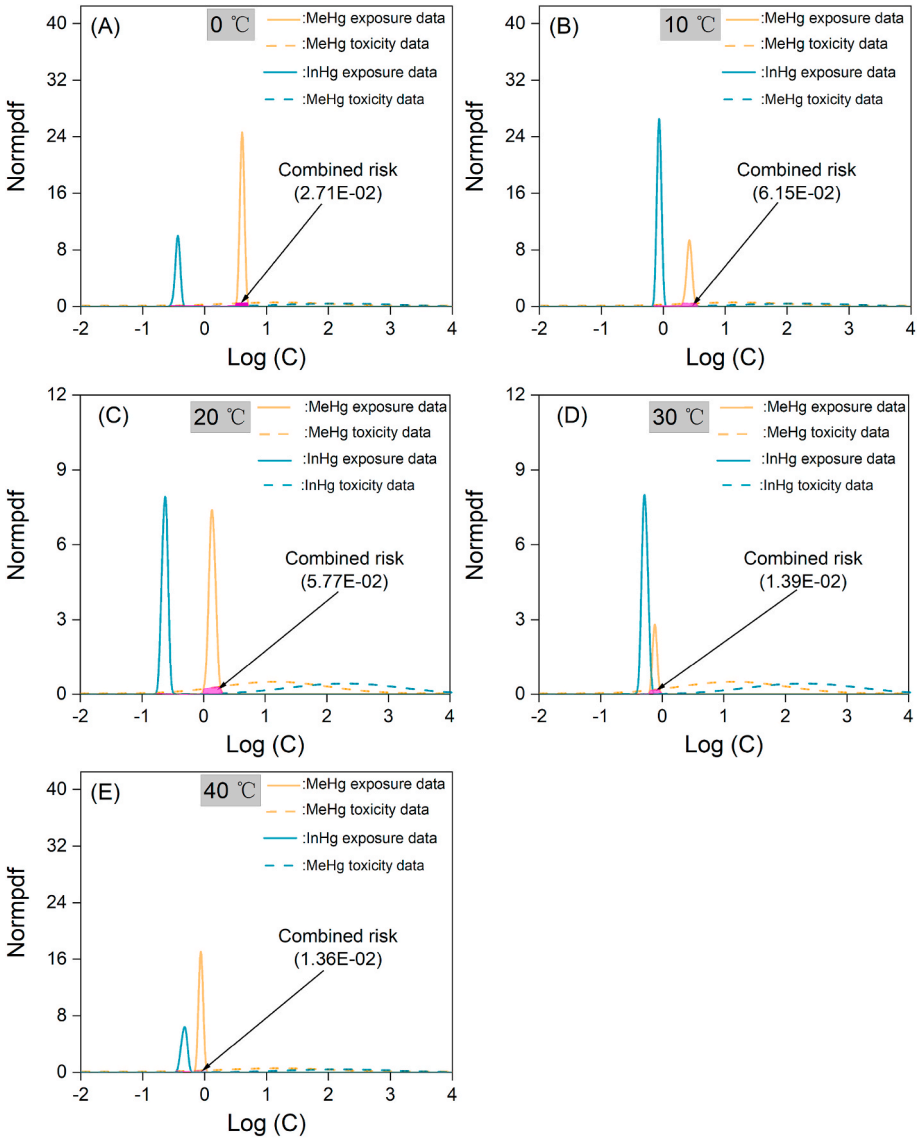

Fig. 5. Joint probabilistic ecotoxicological risk of MeHg and InHg on aquatic biota at 0, 10, 20, 30, and 40 °C, estimated using the SPI model. Pink-shaded areas indicate ecotoxicological risk.

bound forms.

The joint ecological risk profiles reveal that MeHg overwhelmingly governs the temperature dependence of total mercury toxicity, emphasizing its dominant role in mediating ecological outcomes under varying thermal regimes (Fig. 7). This dominance aligns with established toxicokinetic evidence that MeHg is more readily bioaccumulated and biomagnified in aquatic food webs, whereas InHg largely persists in less reactive, sediment-bound states (Mason et al., 1994; Ullrich et al., 2001; Buckman et al., 2019).

From an environmental perspective, the observed nonlinearities carry important implications under ongoing climate warming. Projected increases in sediment temperature in coastal and estuarine systems could transiently amplify MeHg bioavailability and ecological risk before stabilizing or declining beyond thermal thresholds. Such temperature-modulated behavior challenges conventional steady-state assumptions in mercury risk assessment, underscoring the need to incorporate dynamic temperature-dependent parameters into predictive models.

In general, temperature acts as a multifaceted regulator that governs mercury bioavailability through intertwined diffusion–complexation mechanisms (Fig. 7). The integration of DGT-based measurements with probabilistic ecological modeling provides a quantitative framework for predicting thermally mediated variations in mercury toxicity. These insights offer new perspectives for refining ecological risk assessments and for anticipating potential biogeochemical responses of mercury under future climate scenarios.

4.2. *Uncertainty and limitations*

Although the present study provides quantitative insights into temperature-dependent mercury bioavailability and risk dynamics, several sources of uncertainty should be acknowledged.

First, DGT-derived concentrations represent the labile fractions of MeHg and InHg under *in situ* diffusion and resupply conditions. These labile pools may not fully capture the total bioavailable mercury accessible to benthic organisms, especially when strong organic complexation or microbial methylation–demethylation processes occur. Thus, the observed relationships between temperature and DGT-labile mercury species should be interpreted as indicative of potential bioavailability trends rather than absolute exposure levels.

Second, the empirical fitting models (polynomial or nonlinear) inherently simplify complex biogeochemical interactions. Although the

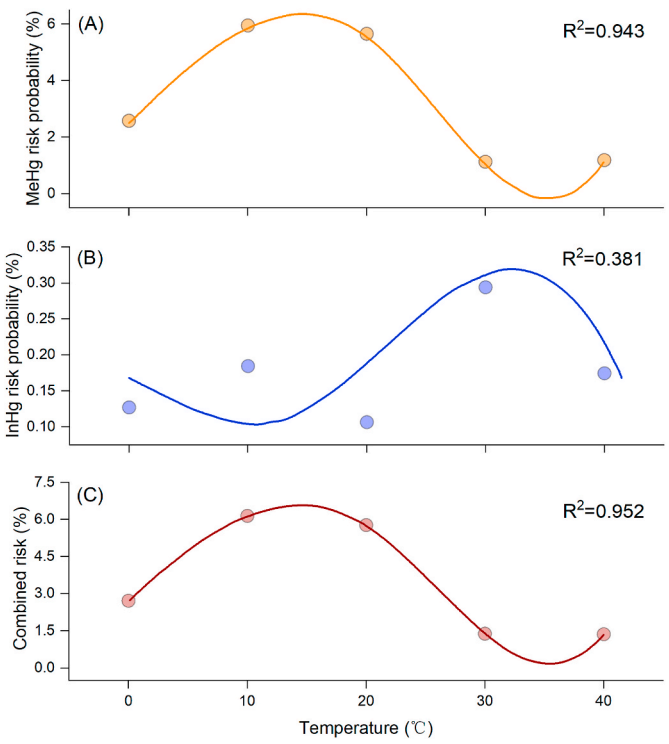

Fig. 6. Temperature-dependent probabilistic ecological risks of (A) methylmercury (MeHg), (B) inorganic mercury (InHg), and (C) their combined effects on aquatic biota in coastal sediments.

high coefficients of determination (R^2) support the statistical robustness of these fits, they reflect correlative rather than mechanistic relationships. Extrapolating beyond the observed temperature range (0–40 °C) should therefore be approached with caution.

Third, environmental variables co-varying with temperature—such as redox potential, organic matter content, and microbial activity—were not explicitly decoupled in this study. These factors may partially confound the apparent temperature effects on mercury speciation and mobility. Future experiments designed to isolate thermal influence from other biogeochemical drivers would strengthen mechanistic understanding of temperature control.

Finally, the probabilistic ecological risk model relies on input distributions derived from limited datasets and on threshold parameters from existing literature. This parameterization inevitably introduces statistical uncertainty, particularly for low-probability or extreme scenarios. Expanding datasets through long-term field observations and incorporating species-specific sensitivity distributions would enhance model robustness.

Despite these limitations, the integrated DGT–probabilistic framework developed here provides a valuable diagnostic approach for assessing thermally modulated mercury risks in dynamic aquatic environments. Continued refinement of this method will improve predictive ecological risk assessment under future climate change scenarios.

4.3. Environmental implications

Climate warming can alter mercury bioavailability and ecotoxicological risks in coastal sediments, yet species-specific responses remain unclear. Using DGT to measure labile methylmercury and inorganic mercury and the SPI probabilistic model for joint risk assessment, this study reveals nonlinear, temperature-dependent effects, with MeHg overwhelmingly dominating total risk. By linking sediment temperature to Hg speciation and ecological outcomes, the work provides a mechanistic, predictive framework for assessing climate-sensitive mercury hazards, informing proactive environmental management and mitigation strategies in coastal ecosystems.

5. Conclusion

This study demonstrates that sediment warming exerts nonlinear, species-specific effects on the bioavailability and ecotoxicological risks of MeHg and InHg in coastal sediments. Using DGT-based measurements combined with the SPI probabilistic risk model, we show that MeHg overwhelmingly dominates total ecotoxicological risk, while InHg contributes modestly but meaningfully. Temperature influences Hg mobility through coupled diffusion–complexation mechanisms, leading to distinct thermal responses for each species. The integrated DGT–SPI framework provides a mechanistic, predictive tool for assessing temperature-sensitive mercury dynamics, offering critical insights for climate-adaptive risk assessment and environmental management in coastal ecosystems.

CRediT authorship contribution statement

Yang-Guang Gu: Writing – review & editing, Writing – original

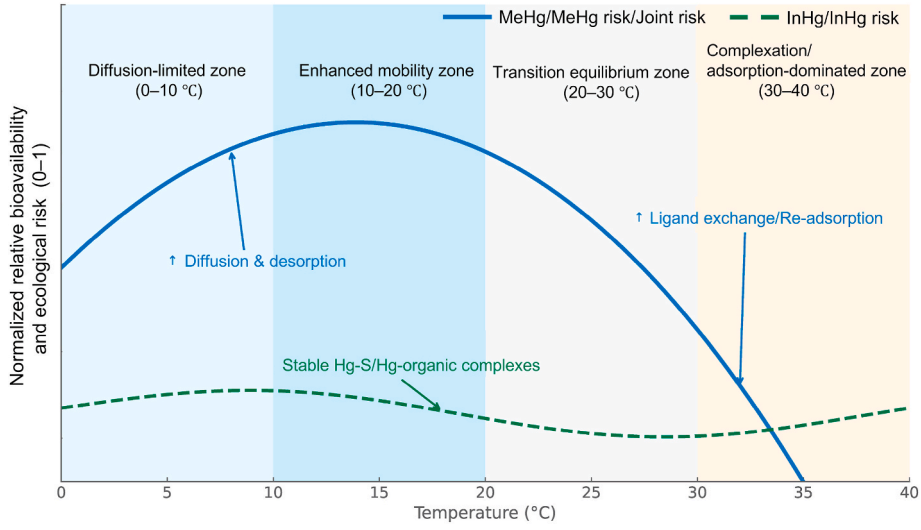

Fig. 7. Conceptual illustration of temperature-modulated mercury bioavailability and ecological risk in sediments. This conceptual graph is based on data from Fig. S3.

draft, Visualization, Validation, Supervision, Software, Resources, Project administration, Methodology, Investigation, Funding acquisition, Formal analysis, Data curation, Conceptualization. **Yanpeng Gao:** Validation, Resources, Methodology, Funding acquisition, Data curation. **Richard W. Jordan:** Writing – review & editing, Validation, Data curation. **Shi-Jun Jiang:** Writing – review & editing, Validation, Data curation.

Declaration of competing interest

The authors declare that they have no known competing financial interests or personal relationships that could have appeared to influence the work reported in this paper.

Acknowledgements

This study was supported by the National Natural Science Foundation of China (42322704, 42277222), National Key R&D Program of China (2022YFC3105600) and Central Public-interest Scientific Institution Basal Research Fund, CAFS (2023TD15).

Appendix A. Supplementary data

Supplementary data to this article can be found online at https://doi.org/10.1016/j.envres.2026.123996.

Data availability

Data will be made available on request.

References

Acquavita, A., et al., 2021. Occurrence and speciation of arsenic and mercury in alluvial and coastal sediments. Current Opinion in Environmental Science & Health 22, 100272.
Bełdowski, J., et al., 2018. Seasonal changes of mercury speciation in the coastal sediments. J. Soils Sediments 18, 3424–3436.
Blanchfield, P.J., et al., 2022. Experimental evidence for recovery of mercury-contaminated fish populations. Nature 601, 74–78.
Bolaños-Alvarez, Y., et al., 2024. Regional assessment of the historical trends of mercury in sediment cores from wider Caribbean coastal environments. Sci. Total Environ. 920, 170609.
Buckman, K.L., et al., 2019. Sediment organic carbon and temperature effects on methylmercury concentration: a mesocosm experiment. Sci. Total Environ. 666, 1316–1326.
Dastoor, A., et al., 2022. Arctic Mercury cycling. Nat. Rev. Earth Environ. 3, 270–286.
Davison, W., Zhang, H., 1994. *In situ* speciation measurements of trace components in natural waters using thin-film gels. Nature 367, 546–548.
Dabré, D., et al., 2025. Mercury transfer and transformation from mine soil to river sediments: the potential role of amorphous iron oxides in methylation processes in southern Burkina Faso. Environ. Sci. Process. Impacts 27, 3246–3260.
Gabriel, M.C., Williamson, D.G., 2004. Principal biogeochemical factors affecting the speciation and transport of mercury through the terrestrial environment. Environ. Geochem. Health 26, 421–434.
Gu, Y.G., et al., 2022a. Risk assessment of heavy metal and pesticide mixtures in aquatic biota using the DGT technique in sediments. Water Res. 224, 119108.
Gu, Y.G., et al., 2020. First attempt to assess ecotoxicological risk of fifteen rare earth elements and their mixtures in sediments with diffusive gradients in thin films. Water Res. 185, 116254.
Gu, Y.G., et al., 2025a. Overlooked combined ecotoxicological risk of naturally occurring beryllium and thallium in sediments to aquatic biota: an SPI model-based assessment in the pearl river Estuary. ACS ES&T Water 5, 5145–5156.
Gu, Y.G., et al., 2022b. Appraising ecotoxicological risk of mercury species and their mixtures in sediments to aquatic biota using diffusive gradients in thin films (DGT). Sci. Total Environ. 825, 154069.
Gu, Y.G., et al., 2023. Nonmetric multidimensional scaling and probabilistic ecological risk assessment of trace metals in surface sediments of Daya Bay (China) using diffusive gradients in thin films. Sci. Total Environ. 867, 161433.
Gu, Y.G., et al., 2025b. Impact of coastal industrialization and urbanization on marine phosphorus cycle: insights from Daya Bay and Zhelin Bay. Gondwana Res. 140, 81–88.
Gu, Y.G., et al., 2012. Multivariate statistical and GIS-based approach to identify source of anthropogenic impacts on metallic elements in sediments from the mid Guangdong coasts, China. Environ. Pollut. 163, 248–255.
Gu, Y.G., et al., 2026. Rising temperatures decrease rare earth element bioavailability and ecological risk in coastal sediments. Environ. Chem. Lett. 24, 21–25.
Haitzer, M., et al., 2002. Binding of mercury(II) to dissolved organic matter: the role of the mercury-to-DOM concentration ratio. Environ. Sci. Technol. 36, 3564–3570.
Harding, G., et al., 2018. Bioaccumulation of methylmercury within the marine food web of the outer Bay of Fundy, Gulf of Maine. PLoS One 13, e0197220.
Helmrich, S., et al., 2022. Critical review of mercury methylation and methylmercury demethylation rate constants in aquatic sediments for biogeochemical modeling. Crit. Rev. Environ. Sci. Technol. 52, 4353–4378.
Jonsson, S., et al., 2017. Terrestrial discharges mediate trophic shifts and enhance methylmercury accumulation in estuarine biota. Sci. Adv. 3, e1601239.
Lan, R., et al., 2025. Tracing mercury sources and transfer pathways in Pacific and Atlantic Ocean tuna and billfish using mercury stable isotopes. J. Hazard Mater. 496, 139189.
Lavergne, C., et al., 2025. Unveiling hidden mercury and methylmercury sources: the role of submarine groundwater discharge in coastal lagoons. Environ. Sci. Technol. 59, 20653–20664.
Li, C.J., et al., 2025a. Aligning global mercury mitigation with climate action. Nat. Commun. 16, 7826.
Li, Z.B., et al., 2025b. Genomic potential for mercury biotransformation in marine sediments across marginal slope to hadal zone. Nat. Commun. 16, 8655.
Liem-Nguyen, V., et al., 2017. Thermodynamic stability of mercury(II) complexes formed with environmentally relevant low-molecular-mass thiols studied by competing ligand exchange and density functional theory. Environ. Chem. 14, 243–253.
Mason, R.P., et al., 1994. The biogeochemical cycling of elemental mercury: anthropogenic influences. Geochem. Cosmochim. Acta 58, 3191–3198.
Méndez-López, M., et al., 2025. Mobilization of mercury by sediment transport after a prescribed fire in NE Portugal: insight into size classes and temporal variation. J. Hazard Mater. 484, 136657.
Man, X.T., et al., 2022. Anthropogenic impacts on the temporal variation of heavy metals in Daya Bay (South China). Mar. Pollut. Bull. 185, 114209.
Man, X.T., et al., 2025. Centennial-scale evolution, source apportionment, and ecological risks of heavy metals in Daya Bay, South China sea. Environ. Pollut. 382, 126768.
Miller, C.L., et al., 2009. Kinetic controls on the complexation between mercury and dissolved organic matter in a contaminated environment. Environ. Sci. Technol. 43, 8548–8553.
OECD (Organisation for Economic Co-operation and Development), 2017. Guidance on the Incorporation of Bioavailability Concepts for Assessing the Chemical Ecological Risk and/or Environmental Threshold Values of Metals and Inorganic Metal Compounds. Series on Testing & Assessment OECD Publishing, Paris. https://doi.org/10.1787/9789264274839-en.
Olsen, T.A., et al., 2018. Kinetics of methylmercury production revisited. Environ. Sci. Technol. 52, 2063–2070.
Park, J.-D., Zheng, W., 2012. Human exposure and health effects of inorganic and elemental mercury. Journal of preventive medicine and public health 45, 344.
Pi, K., et al., 2020. Direct measurement of aqueous mercury(II): combining DNA-based sensing with diffusive gradients in thin films. Environ. Sci. Technol. 54, 13680–13689.
Ravichandran, M., 2004. Interactions between mercury and dissolved organic matter—a review. Chemosphere 55, 319–331.
Ren, M.Y., et al., 2018. Development of a new diffusive gradient in the thin film (DGT) method for the simultaneous measurement of CH3Hg+ and Hg2+. New J. Chem. 42, 7976–7983.
Rosati, G., et al., 2024. Mercury cycling in contaminated coastal environments: modeling the benthic-pelagic coupling and microbial resistance in the Venice Lagoon. Water Res. 261, 121965.
Saiz-Lopez, A., et al., 2025. Role of the stratosphere in the global mercury cycle. Sci. Adv. 11.
Semenzin, E., et al., 2008. Integration of bioavailability, ecology and ecotoxicology by three lines of evidence into ecological risk indexes for contaminated soil assessment. Sci. Total Environ. 389, 71–86.
Ullrich, S.M., et al., 2001. Mercury in the aquatic environment: a review of factors affecting methylation. Crit. Rev. Environ. Sci. Technol. 31, 241–293.
Wang, Q.Y., et al., 2020. Rates and dynamics of Mercury isotope exchange between dissolved elemental Hg(0) and Hg(II) bound to organic and inorganic ligands. Environ. Sci. Technol. 54, 15534–15545.
Zhang, H., Davison, W., 1995. Performance characteristics of diffusion gradients in thin films for the in situ measurement of trace metals in aqueous solution. Anal. Chem. 67, 3391–3400.
Zhong, M.F., et al., 2025. Climate-driven deoxygenation promoted potential mercury methylators in the past Black sea water column. Nat. Water.